



An optimization method for material sound absorption performance based on surrogate model

Hao Song^{1,*}, Lin Su¹, Xiaowei Yan¹, and Jinshi Liu²

¹Systems Engineering Research Institute, Beijing 100036, China

²School of Naval Architecture and Ocean Engineering, Jiangsu University of Science and Technology, Zhenjiang 212000, China

Received 13 July 2021, Accepted 6 April 2022

Abstract – In some complex engineering design problems, the use of numerical simulation methods to solve the target value often consumes several hours or even longer, which limits the real-time response to the model. The surrogate model can solve the above-mentioned shortcomings because of its use of statistical ideas to link the design variables with the target value. Kriging model has been widely used in other fields due to its simple algorithm compilation and good stability of calculation results, but there is little research in the field of silencing structure optimization. In order to study the optimization efficiency and optimization effect of the surrogate model in the optimization design of the anechoic structure, combined with the surrogate model and the multi-point plus point criterion, a set of general optimization algorithm framework suitable for the surrogate model and the gradient-enhanced Kriging model (GEK) was developed. Based on this framework, the evolution of the sound absorption coefficient of the anechoic structure under three different working conditions (100–10 000 Hz, 100–1500 Hz, 100–10 000 Hz frequency under static pressure) was compared. The gradient enhancement Kriging model and the gradient optimization algorithm were compared and studied. The results show that under the assumption that the gradient of the objective function and the objective function have the same amount of calculation, the optimization times obtained by the Kriging model with gradient enhancement are better than those obtained by the Kriging model and the gradient optimization algorithm in most cases, and the optimization results of GEK and Kriging models are better than those of gradient optimization.

Keywords: Surrogate model, Kriging model, Gradient-enhance Kriging, Optimal design of anechoic coating

1 Introduction

Acoustic stealth performance is currently one of the most important combat effectiveness indicators for underwater target structures. Covering the shell of the underwater target structure with a layer of sound-absorbing material can weaken the echo signal of the active sonar and reduce the noise radiated by the underwater target structures [1]. The essence of sound-absorbing materials is to add particles such as cavities [2–4] and metal balls [5, 6] into viscoelastic materials such as rubber. In the resonance scattering frequency band of the particles, the scattering of sound waves propagating in the sound-absorbing layer is enhanced. The wave is largely dissipated due to the influence of the damping effect of the matrix, so that the sound absorption performance of the sound absorption layer in this frequency band is significantly improved.

A common method to evaluate the sound absorption performance of materials is to analyze their acoustic

properties. At present, this is mainly performed using analytical methods [7–10] or numerical methods [11–15]. The analytical methods refer to the equivalent treatment of the acoustic parameters (such as wave speed, density, etc.) of the sound absorber according to the wave theory in the layered medium, to obtain the analytical solution of the sound absorption coefficient of the sound absorber. Numerical methods refer to the meshing of sound-absorbing structure and surrounding environment (water and rigid liner) with finite element. This is combined with boundary element, related control equations, and numerical calculation of sound-structure coupling, to obtain the acoustic performance of the sound-absorbing body. However, whether it is an analytical model or a numerical model, there is a complicated functional relationship between the physical and structural parameters of the sound-absorbing body and its acoustic performance. According to the requirements of different acoustic performances, by optimizing the structure or material properties of the sound absorber, the required needs of acoustic materials and structures can be obtained, such as in [2, 6, 12].

*Corresponding author: songhaox@163.com

In recent decades, optimization methods have been extensively studied in the field of acoustic materials properties. Gerstoft [16] used synthetic wavenumber data to propose multi-parameter inversion of wave speed and layer thickness of the horizontal layered seafloor. Monte Carlo genetic algorithm is used to solve the optimization problem. Westerlin [17] simulated the pressure field in the standard factory building and used the geoacoustic parameter inversion method to perform geometric harmonic parameter matching field inversion. Ivansson [18] studied the acoustic reflection of a rubber anechoic layer with periodically distributed spherical cavities. Using a forward model based on the Riccati method and a specific multiple scattering and global optimization method, the anechoic layer was designed with a wide sound frequency band. Chang et al. [19] used simulated annealing algorithm to optimize the perforation rate and thickness of a composite muffler containing a perforated plate. Tao et al. [20] used genetic algorithms to conduct a multi-parameter comprehensive optimization study on the physical properties and structural dimensions of the sound-absorbing material.

Generally, the existing optimization models were based on complex algorithms and finite element calculations, which have a large amount of calculation and poor repeatability. In addition, the model results cannot be calculated in time. In order to reduce the amount of calculation and complexity in engineering optimization, approximation methods are often used to establish approximate models. Approximation approaches are essentially the construction of approximation functions, which separate complex subject analysis from the optimization process for optimization. After that, the approximate optimal solution of the actual problem is obtained [21–25]. The approximation method only needs to perform a limited number of calculations, and then approximate these data to obtain an approximate model. In each subsequent calculation and simulation, only the constructed approximate model is needed to be called directly, which reduces the calculation time and meet the accuracy requirements of the calculation results. Kriging model is an unbiased estimation model based on a random process with the smallest estimation variance. Compared with other proxy models, the algorithm is simple to write and the calculation results are relatively stable. It has been widely used in environmental science, meteorology, hydrogeology, and other fields [26, 27]. However, it has not been used in the field of hydroacoustic, so whether it can be used in the field of acoustics and noise reduction of underwater target structures to improve structure optimization efficiency and optimization effects has not yet been investigated. Therefore, in order to reduce the amount of calculation and complexity in engineering optimization to achieve the purpose of rapid calculation of optimization results. This paper intends to investigate optimization methods for materials sound absorption performance based on a surrogate model, and evaluate each method effectiveness in sound absorption performance. At the same time, it compares with the existing optimization models, analyzes its advantages, and disadvantages, and finds the optimal

material optimization method suitable for anechoic structure.

2 Optimized design method for noise reduction of acoustic overlay based on surrogate model

2.1 Surrogate model approach

The surrogate model refers to the process of establishing a mathematical approximate model to replace the original complex model to solve the analysis based on mathematical statistics theory. it uses the known sample point information, and under the premise of ensuring the accuracy of the sample. Figure 1 shows a schematic diagram of the general agent model construction. It can be seen from the figure that the surrogate model technology mainly includes two aspects: (1) Based on the experimental design method, input the scale of the sample point and the position of the sample point in the variable space, and then use the numerical simulation model to calculate the output of the variable value. (2) Substitute the input variables and output variables into the agent model, train to obtain the approximate agent model, and complete the construction of the agent model.

2.2 Choice of surrogate model

The core content of surrogate model technology is to extract experimental design sample points in the input variable space x . Obtain the corresponding observation value of each sample point through physical experiment or computer simulation analysis, and construct an approximate surrogate model through the known training sample data set to realize the output variable. The functional relationship between y and the input variable x is approximated.

The Kriging model was first proposed by South African geologist Krige [21] in 1951. It is an unbiased estimation model based on a random process with the smallest estimation variance. In the late 1980s, Sacks [22] and others studied computer experimental analysis and design technology based on the Kriging model, and applied the Kriging model to deterministic calculations or interpolation approximation of experimental data, which greatly promoted the Kriging model in engineering field of application. Subsequently, the Kriging model has been widely used in many fields such as environmental science, meteorology, hydrogeology, geographic information systems, aviation, aerospace, and automobiles. Based on the Kriging model, the Co-Kriging model, the gradient-enhanced Kriging model [28], and the variable credibility Kriging model [29] was developed [30]. The most used are the Kriging model and the Kriging model with gradient enhancement.

2.2.1 Kriging surrogate model

In the Kriging model, for the m -dimensional problem, if the objective function (or state variable) is sampled to

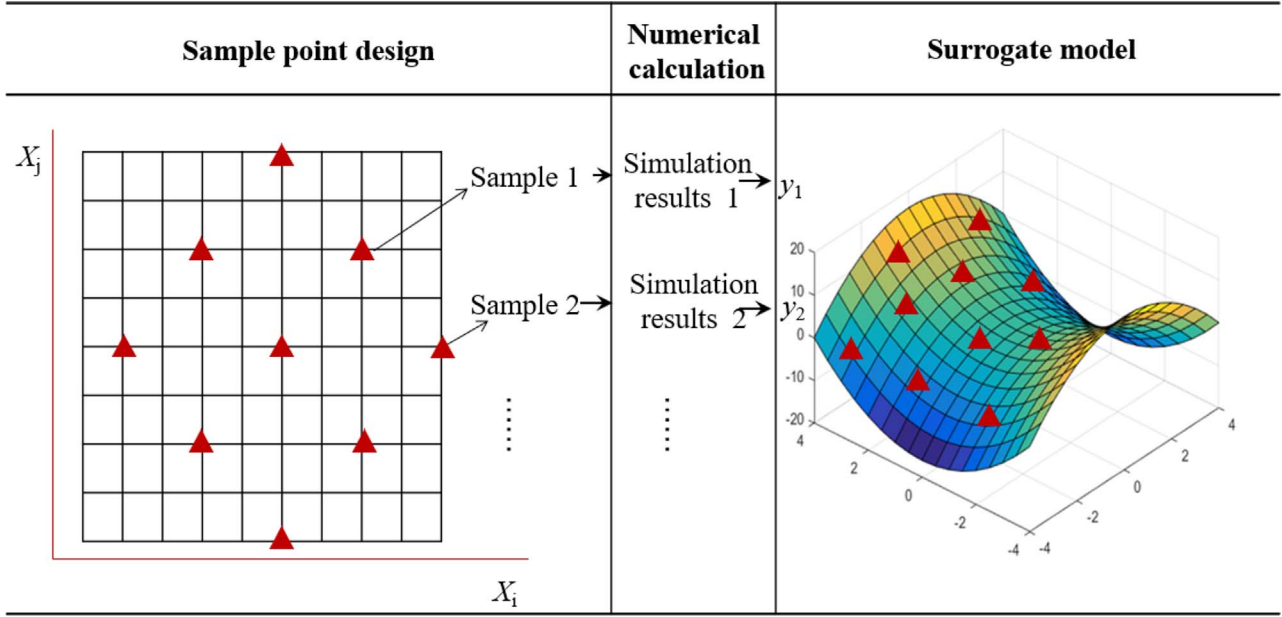


Figure 1. Typical surrogate modeling method.

obtain n function values, the sampling location and the corresponding sample point response value can be written as:

$$\mathbf{S} = \begin{bmatrix} \mathbf{x}^{(1)} \\ \mathbf{x}^{(2)} \\ \dots \\ \mathbf{x}^{(n)} \end{bmatrix} = \begin{bmatrix} x_1^{(1)} & x_2^{(1)} & \dots & x_m^{(1)} \\ x_1^{(2)} & x_2^{(2)} & \dots & x_m^{(2)} \\ \dots & \dots & \ddots & \dots \\ x_1^{(n)} & x_2^{(n)} & \dots & x_m^{(n)} \end{bmatrix} \in \mathbf{R}^{n \times m}, \quad (1)$$

$$\mathbf{y}_S = [y^{(1)}, \dots, y^{(n)}]^T \in \mathbf{R}^n, \quad (2)$$

where: S is the sample matrix, each row represents a sample point; y_S is the column vector, and each element represents a function value of a sample point. The purpose of establishing an approximate model is to use the known sample data (S , y_S) to obtain the predicted value at any unknown point.

Introducing statistical assumptions, for any position x , the corresponding function value $y(x)$ is replaced by a random function $Y(x)$, and $y(x)$ is only one of the possible results of $Y(x)$:

$$Y(x) = \sum_{j=1}^k \beta_j f_j(x) + Z(x), \quad (3)$$

where: $f_j(x)$ is the basic function, β_j is the corresponding coefficient, $\sum_{j=1}^k \beta_j f_j(x)$ represents the mathematical expectation of $Y(x)$. $Z(x)$ is a static random process with a mean value of zero and a variance of σ_Z . Among them, the random function covariance can be expressed as:

$$\text{Cov}[Z(x), Z(x')] = \sigma_Z^2 R(x, x'), \quad (4)$$

where $R(x, x')$ is the “correlation function” (only related to spatial distance), which represents the correlation between random variables at different positions, and satisfies the following: $R = 1$ when the distance is zero, $R = 0$ when the distance is infinite; R decreases as the distance increases.

The Kriging model is an unbiased estimation model with the smallest estimated variance. Lagrangian multiplier and maximum likelihood estimation methods were used to obtain the minimum variance of the model, which can be expressed as:

$$\hat{y}(x_0) = \hat{\beta} + r^T(x_0)R^{-1}(\mathbf{Y} - \mathbf{I}\hat{\beta}), \quad (5)$$

where: I is the unit column vector, $\hat{\beta} = (\mathbf{I}^T \mathbf{R}^{-1} \mathbf{Y})^T (\mathbf{I}^T \mathbf{R}^{-1} \mathbf{I})^{-1}$, $\hat{\sigma}^2 = 1/[(\mathbf{Y} - \mathbf{I}\hat{\beta})^T \mathbf{R}^{-1} (\mathbf{Y} - \mathbf{I}\hat{\beta})]$ is the variance, and $\hat{\sigma}$ is the prediction standard deviation.

2.2.2 Gradient enhanced Kriging model (GEK)

The GEK model is developed based on the Kriging model. Its ideas, principles and modeling methods are basically the same as the Kriging model, except that not only the function value at the sample point is used in the model, but also the gradient value at the sample point is used. The following introduces a direct GEK model developed by Han et al. [28].

For GEK, the response value column vector of the above sample data is expanded, and the gradient information at the sample point is added to the response value in the form of partial derivative. Then the sample and response value matrix with gradient information are extracted as:

$$\mathbf{y}_S = [y^{(1)}, \dots, y^{(n)}, \partial y^{(1)}, \dots, \partial y^{(n)}]^T \in \mathbf{R}^{n+n'}. \quad (6)$$

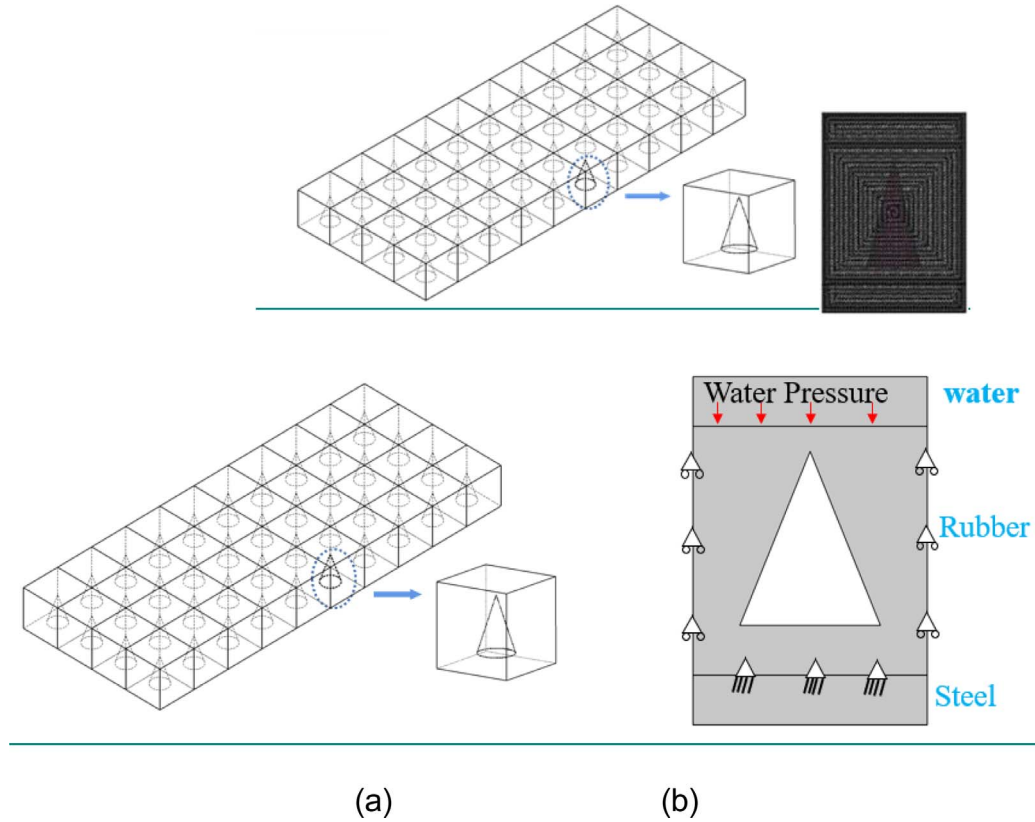


Figure 2. Schematic diagram of anechoic structure. (a) Acoustic covering layer unit cell; (b) mesh analysis.

The predicted value of the unknown function by the GEK model is defined as the weighting of all sampling function values and all sampling partial derivative values, namely:

$$\hat{y}(x) = \sum_{i=1}^n w^{(i)} y^{(i)} + \sum_{j=1}^{n'} \lambda^{(j)} \partial y^{(j)}, \quad x \in \mathbf{R}^m. \quad (7)$$

Similar to the derivation process of the Kriging model, the predicted value of the GEK model can be obtained by:

$$\hat{y}(x) = \beta_0 + \mathbf{r}^T(\mathbf{x})\mathbf{R}^{-1}(\mathbf{y}_s - \beta_0\mathbf{F}), \quad (8)$$

where: $\mathbf{F} = [1 \dots 10 \dots 0]^T$; $\beta_0 = (\mathbf{F}^T \mathbf{R}^{-1} \mathbf{F})^{-1} \mathbf{F}^T \mathbf{R}^{-1} \mathbf{y}$.

2.3 Numerical calculation of anechoic structure

Since the cavity structure is periodically and uniformly distributed in the acoustic covering layer, as shown in Figure 2. In order to simplify the calculation, according to the Bloch theorem of the periodic structure, only the smallest unit is analyzed, and the covering layer is calculated in the infinite water and rigid backing under the sound absorption performance [31].

The sound absorption performance of the complex-shaped cavity acoustic covering layer analytical calculation can no longer give a more accurate solution, and finite element simulation is required. In this article, the numerical calculation software uses COMSOL Multiphysics. When the vertically incident elastic wave propagates along the

cylindrical axis, the change in the axial angle is not considered. The top finite water layer simulates an infinite fluid domain, the middle covering layer contains a cavity containing air, and a steel material is used as a rigid backing. The incident wave sound pressure p_i of the acoustic covering layer can be expressed as:

$$p_i = \frac{p_2 - p_1 e^{jkd}}{e^{-jkd} - e^{jkd}}. \quad (9)$$

In the formula, k is the wave number. The sound pressure reflection coefficient is:

$$R_{re} = \frac{p_r}{p_i}. \quad (10)$$

According to the sound pressure reflection coefficient of the sample R_{re} , the sound absorption coefficient of the sample α is obtained by:

$$\alpha = 1 - |R_{re}|^2. \quad (11)$$

The specific geometry of the model is: The width of the model is 50 mm, the height of the water is 10 mm, and the rigidity is 5 mm. The boundary conditions of the model are shown in Figure 2b, and the specific settings are as follows: the upper part of the model is infinite water, and the top is the plane wave radiation condition. Because the sound-absorbing cover layer is fixedly connected to the surface of the steel layer, the contact surface adopts fixed

Table 1. Model material parameter table.

Material type	Density (kg/m ³)	Young's modulus (GPa)	Poisson's ratio	Loss factor
High polymer elastic rubber	1300	0.4	0.49	0.6
Stainless Steel Grade 304 (UNS S30400)	7850	190	0.28	–
Water	1000	–	–	–

constraint conditions and the two sides are periodic boundaries. The mesh analysis of the cavity adopts a hexahedral grid, and the maximum grid size is 0.1 mm. The relevant materials parameters used in the simulation are all drawn from the literature and shown in Table 1 below [32, 33].

The sound velocity in water is 1489 m/s, and the initial incident sound pressure is 1 Pa. The existing calculation results show that when the calculation frequency is less than 10 000 Hz, the sound absorption coefficient is low and the structure needs to be further optimized. Therefore, the calculation frequency range of this study is 100–10 000 Hz. At the same time, with the continuous development of sonar technology to low frequencies, in order to ensure the advanced nature of the technical sound-absorbing structure, this paper also considers the optimization of acoustic sound-absorbing materials in the low-frequency range (100–1500 Hz). Therefore, this study finally chooses two frequency ranges to optimize: 100–10 000 Hz and 100–1500 Hz.

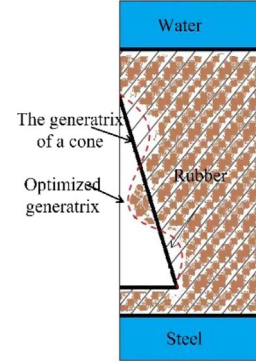
2.4 Design space of anechoic structure

The internal cavity schematic diagram of the anechoic structure is shown Figure 3. The essence is to embed periodically distributed spherical, cylindrical air cavity or hardware material in the viscoelastic material layer with high damping. Different conical busbar structures have an important influence on the sound absorption capacity of the material. Studies have shown that the performance of the cavity-type sound-absorbing cover layer is greatly affected by its internal cavity structure (hole shape, size and arrangement, etc.). The sound absorption performance of the cover layer structure can be effectively improved by rationally designing the cavity structure configuration. In the optimization calculation, the change of the cavity structure configuration is mainly realized by controlling the shape parameter curve. At present, there are few mature curves describing the cavity structure, so this study takes the optimization of the conical bus as an example to explore the optimization effect of the proxy model in the cavity structure optimization calculation.

The optimized bus is based on the Burns polynomial, and the expression of the deviation function is as follows:

$$\Delta y = \sum_{i=1}^N Q_i y^i (1-y)^{N-i}. \quad (12)$$

Since the value of N in the deviation function is an infinite number of items, considering the optimization results and the amount of calculation comprehensively, $N = 7$ is initially selected.

**Figure 3.** Schematic diagram of the anechoic internal cavity.**Table 2.** Constraints of 10 optimization parameters.

Optimizing parameters	Lower limit	Upper limit
Q_1	0	1
Q_2	0	1
Q_3	0	1
Q_4	0	1
Q_5	0	1
Q_6	0	1
Q_7	0	1
E	10 [MPa]	100 [MPa]
ν	0.48	0.498
η	1.1	1.9

Beside the influence of geometric structure on sound absorption performance, the influence of material parameters is also considered. Studies have shown that the Young's modulus, Poisson's ratio, and hydrostatic pressure of the material affect the sound absorption performance [34]. Therefore, the design space in this paper is a 10-parameters high-dimensional space. The constraints formed by each parameter are shown in Table 2.

2.5 Sample point design and point addition criteria of anechoic structure

2.5.1 Sample point design of anechoic structure

Experiment design is a mathematical method based on probability theory, mathematical statistics, and linear algebra. The method scientifically arranges experiment content and analyze experiment results. As an important part of the surrogate model, the main purpose of experimental design is to efficiently select sample points in the entire variable space. This is to reflect as much as possible the change characteristics of the input variable space with a limited

sample point scale, to ensure accuracy, and reduce the effect of sample points.

Latin hypercube sampling design is a type of test design specially proposed for simulation test. It is a space-filled design, so that the input combination fills the entire test interval relatively evenly, and each variable is used once at any level. Figure 4 shown the space filling comparison of several commonly used sampling. It could be seen that, compared with other test methods, the Latin hypercube design has a better space filling ability, to realize the use of the same data point to study more data combinations.

In Latin hypercube design, assuming there are r factors in the design problem, each factor is divided into n intervals, then each factor has n level values. The Latin hypercube design table is a $n \times r$ matrix composed of n level values of r factors. In this study, the impact of 10 parameters on sound absorption performance is studied. The study includes 10 factors in total, and in order to make the surrogate model more accurate, each factor is divided into 30 intervals, so there are 30 levels.

2.5.2 Pointing guidelines

Although the Kriging model has a good global approximation ability, it cannot find the optimal value in the design space only by relying on the initial sample information. Therefore, it is necessary to add new sample points to find the true optimal value and improve the accuracy of the Kriging model. This study intends to adopt the objective function maximum criterion with good local convergence and the EI maximum criterion with good global convergence.

1. Maximum objective function criterion

The surrogate model is considered accurate enough to directly find the maximum value of the objective function on the surrogate model, that is, after the surrogate model is established, the following sub-optimization problems are solved:

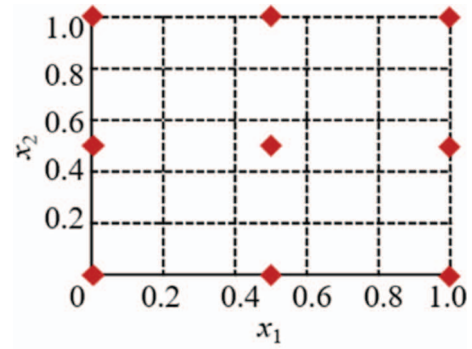
$$\text{maximum} : \hat{y}(x).$$

This criterion does not consider the error of the model. The newly added sample points are mainly concentrated near the current real optimal solution, so it is a local addition criterion.

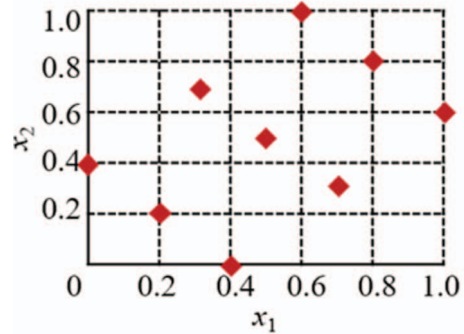
2. EI maximum criterion with good global convergence

Assuming that the optimal objective function value in the sample set is y_{\max} , and the random variable $Y(x)$ obeys the normal distribution with the mean value $y(x)$ and the standard deviation $s(x)$. The relative improvement of the objective function at x is $I = y_{\max} - Y(x) > 0$, so the expected value of I is given by:

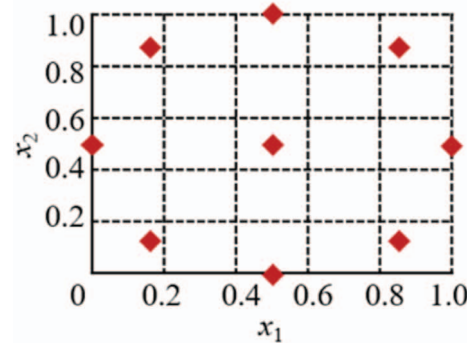
$$E[I(x)] = \begin{cases} (y_{\min} - \hat{y})\Phi\left(\frac{y_{\min} - \hat{y}}{s}\right) + s\varphi\left(\frac{y_{\min} - \hat{y}}{s}\right) & \text{if } s > 0 \\ 0 & \text{if } s = 0 \end{cases} \quad (13)$$



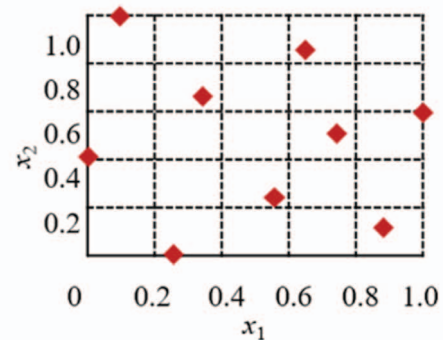
(a)



(b)



(c)



(d)

Figure 4. Comparison of space filling of various sampling methods. (a) 3-level full factorial design; (b) center composite design; (c) uniform design; (d) Latin hypercube design.

The combination of the above two point-adding criteria considers the local convergence and global convergence of optimization. So, it can better apply to local optimization problems and global optimization problems.

2.6 Optimization design method based on surrogate model

The various parts involved in the construction of the surrogate model are described above, including the selection of the surrogate model, the generation of sample points, the solution of response values, and the method of adding points. This section gives the optimization method flow of the surrogate model:

1. Use the experimental design method to generate initial sample points in the design space.
2. Call to construct a numerical model to obtain the response value of each initial sample point. If it is Kriging with gradient enhancement, calculate the gradient of the objective function at the same time.
3. Preliminary establishment of the surrogate model of objective function and constraint function based on sample data, etc.
4. Perform sub-optimization on the surrogate model according to the point-adding criterion.
5. Check whether the best points obtained by the sub-optimization overlap or overlap with the initial sample points. If they are weakly overlapped, eliminate it, and use them as the sample points for verification.
6. Calculate the response value of the added sample point and add it to the sample set.
7. Judge whether the optimization is terminated, otherwise return to (4). If yes, the optimization ends. The flow chart of the optimization process is shown in Figure 5.

3 Shape optimization of acoustic covering layer based on agent model

There are two main indicators for evaluating the pros and cons of an optimization algorithm: optimization efficiency and optimization effect. For optimization efficiency, the time required for optimization should be as short as possible. For optimization effect, it should be as close to or even reach the global optimal solution as possible. In order to compare the application of the two surrogate models, a comparison was conducted under three operational conditions at wide range of frequencies (100–10 000 Hz), low frequency (100–1500 Hz) and full frequency under static pressure.

3.1 Anechoic structure optimization at full frequency

The frequency at which the sound-absorbing structure receives sound waves in water is generally between 100 Hz and 10 000 Hz, and the frequency sampling interval is 100 Hz. The total design parameters are 10 including 7 geometrical parameters and 3 material parameters

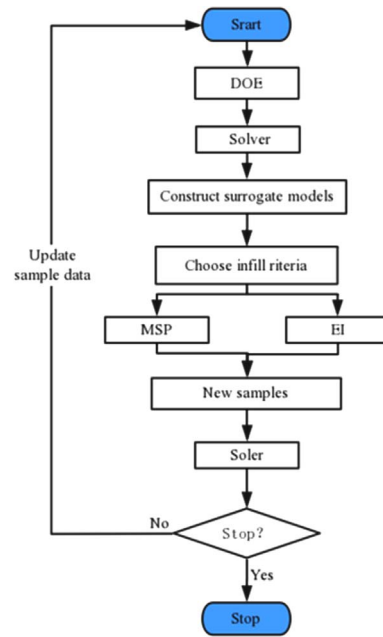


Figure 5. The flow chart of the optimization design method of the surrogate model.

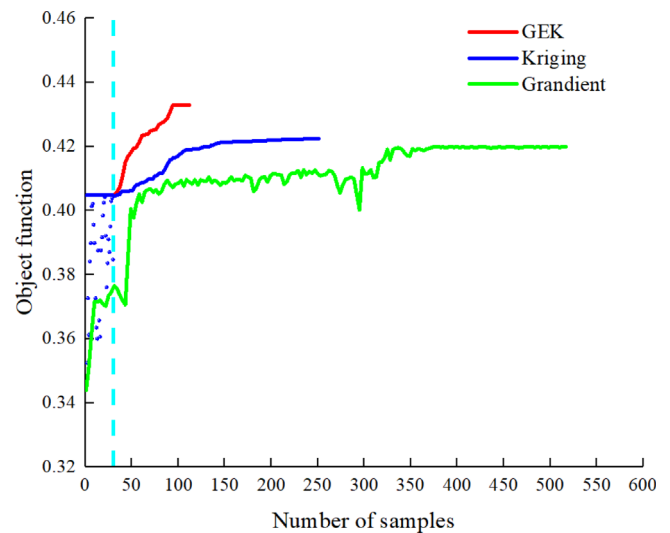


Figure 6. Convergence history of the design objective function at full frequency.

mentioned earlier. The noise reduction coefficient was taken as the optimization target. The mathematical expression of the optimization problem is as follows:

$$\text{maximum: Obj} = \frac{1}{N} \sum_{i=1}^N \alpha(f_i).$$

The specific approach includes using the Latin hypercube algorithm to generate 30 initial samples, and then use finite element software to calculate the response value corresponding to the sample. On this basis, the objective function maximum criterion based on better local convergence

Table 3. Comparison of optimization methods at full frequency.

Optimization method	Optimization target	No. of calculations
Not optimized	0.3440	–
Kriging	0.4224	251
GEK	0.4339	112
Gradient optimization	0.4195	517

Table 4. Parameters of the optimized anechoic structure.

Parameters	Q_1	Q_2	Q_3	Q_4	Q_5	Q_6	Q_7	ν	E	η
Kriging	0.373	0.0165	0.435	0.042	0.615	0.118	0.0384	0.495	100	1.9
GEK	0.3834	0.0175	0.4363	0.0467	0.6264	0.1206	0.0391	0.493	100	1.9
Gradient	0.349	0.108	0.491	0.008	0.033	0.0097	0.0857	0.496	100	1.9

and the EI maximum criterion with better global convergence are used to optimize the selection of points and use them as new sample points for calculation. In addition, the gradient-based optimization algorithm is used as a reference for comparison.

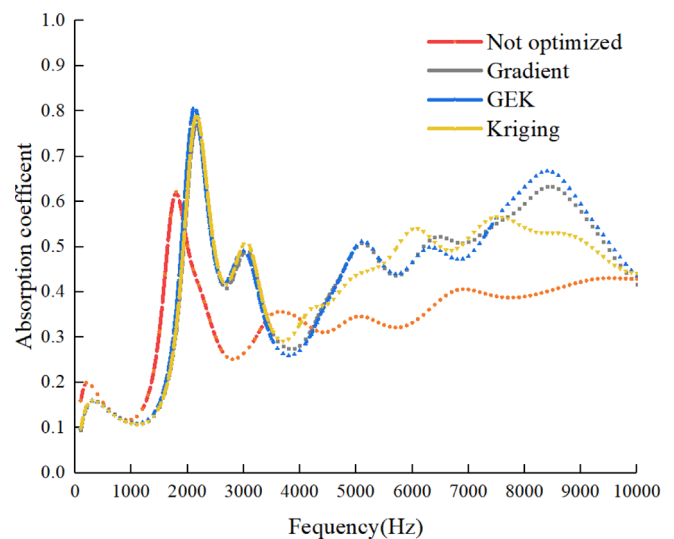
Figure 6 and Table 3 shown the convergence history of the design objective function at full frequency. It could be seen that the number of times the GEK model calls the finite element is less than the Kriging model and less than the gradient optimization algorithm. It shows that the use of gradient information in the surrogate model can improve the accuracy of the surrogate model, so that fewer sample points can be used to lock the best position. The value of each design parameter is shown in Table 4.

Figures 7 and 8 show the comparison diagram of the cavity optimization structure under different optimization parameter values and the corresponding evolution diagram of the noise reduction coefficient with frequency. It can be seen from that the curves obtained by GEK and Kriging optimization are similar but are quite different from the curves of the gradient optimization algorithm. In addition, when the frequency reach more than 2000 Hz, the results of the optimization algorithm can significantly improve the silencing coefficient of the structure, while at 100–2000 Hz, the silencing coefficient of the optimized structure is smaller than that of the unoptimized structure. The reason why the unoptimized result is better than the optimized result is because the objective function in the calculation frequency range (100–10 000 Hz) gives the same weight, and the optimization model looks for the minimum value of the average sound absorption coefficient in the entire calculation frequency range, so it will appear, at some frequencies, the unoptimized result is better than the optimized result.

Comparing different optimization algorithms, the optimization results of the GEK agent are similar to the Kriging optimization, and are better than the results of the gradient optimization algorithm.

3.2 Anechoic structure optimization at low frequency

The sound waves emitted by active sonar are constantly low-frequency [30]. However, many sound-absorbing

**Figure 7.** Sound absorption coefficient curves of different optimization models at full frequency.

materials and structures have low sound-absorbing coefficients in the low-frequency region and have high reflectivity. Therefore, it is necessary to study the optimization of sound-absorbing structures at low frequencies. The frequency selection range is 100–1500 Hz, and the specific optimization method is similar to the noise reduction structure at full frequency. The convergence history and sound absorption curve are shown in Figures 9 and 10, respectively.

Comparing Figures 6 and 9, it could be seen that the number of samples required for optimization at low frequency and full frequency is basically the same and the rules are consistent: $GEK < Kriging < gradient$ algorithm. Figure 10 shown the noise reduction coefficient diagrams of different optimization methods. It could be seen that in terms of the maximum optimization goal: $Kriging > GEK > gradient$ algorithm. In terms of the distribution characteristics of the sound absorption coefficient, GEK and Kriging have obvious optimization effects at 1000–1500 Hz, while the gradient optimization algorithm has more obvious optimization effects at 100–1000 Hz.

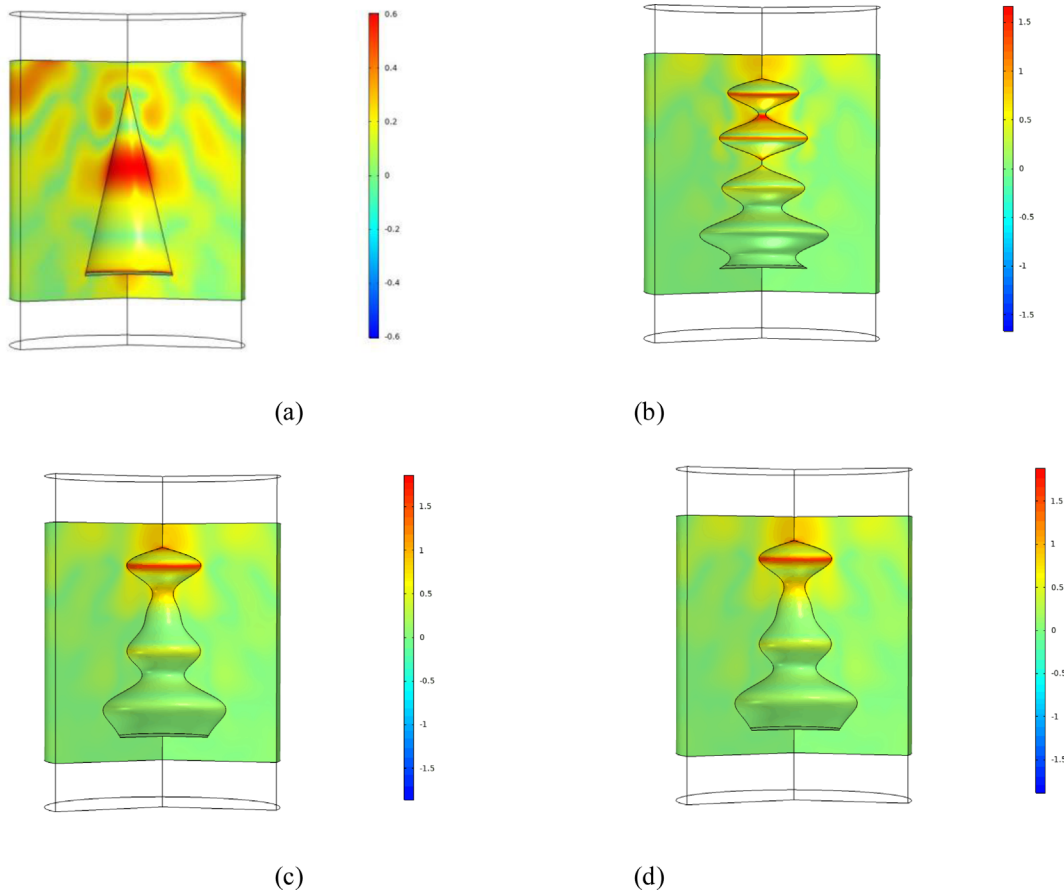


Figure 8. Stress distribution under different optimized parameter values. (a) Not optimized; (b) Gradient; (c) GEK; (d) Kriging.

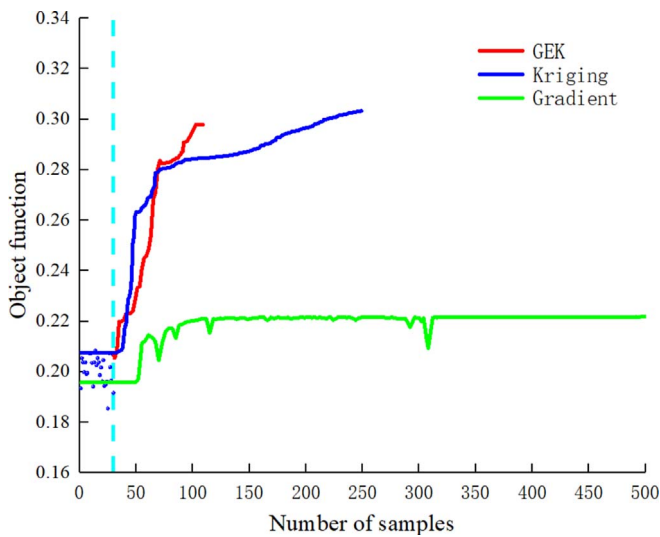


Figure 9. Convergence history of design objective function at low frequency.

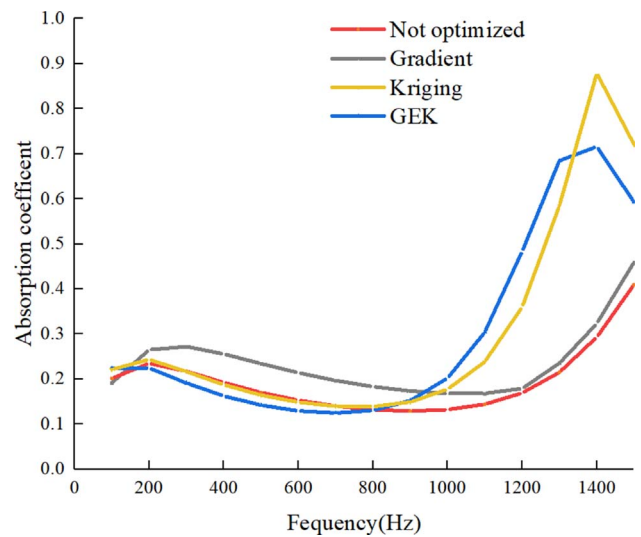


Figure 10. Sound absorption coefficients of different optimization models at low frequencies.

This occurs because the GEK and kriging algorithms are optimization algorithms based on surrogate models. Through appropriate addition criteria, the global optimization can be satisfied. However, due to the defects of the

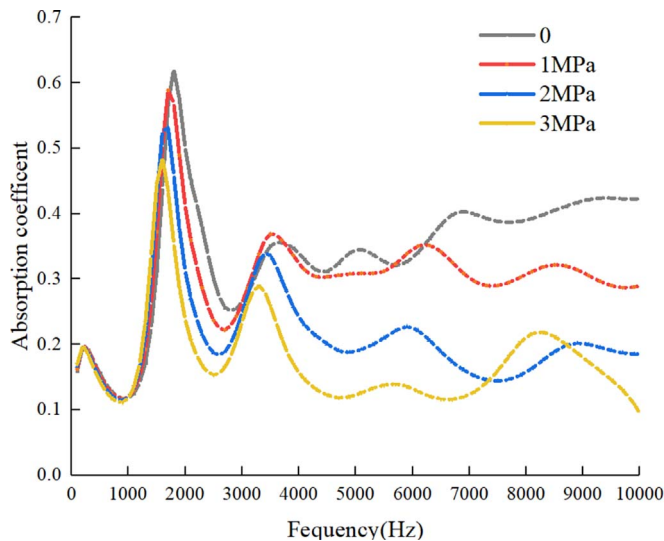
algorithm itself, the gradient optimization algorithm is easy to fall into local optimization rather than global optimization. Therefore, the final optimization result is worse than the other two. At the same time, the GEK model adds

Table 5. Comparison of optimization methods at full frequency.

Optimization method	Optimization goal	No. of calculations
Not optimized	0.1958	–
Kriging	0.3048	249
GEK	0.2978	109
Gradient optimization	0.2348	562

Table 6. The value of each design parameter in the final optimization model at low frequency.

Parameters	Q_1	Q_2	Q_3	Q_4	Q_5	Q_6	Q_7	ν	E	η
Kriging	0.0992	0.2184	0.1292	0.0580	0.3893	0.2389	0.0698	0.494	5.84	1.9
GEK	0.1365	0.0798	0.4306	0.0834	0.7667	0.0197	0.1685	0.495	5.06	1.9
Gradient	0.2687	0.1854	0.1032	0.6094	0.0226	0.3565	0.0282	0.496	4.96	1.9

**Figure 11.** Sound absorption coefficient under different static pressures.

gradient information based on the kriging model, so it needs less times to reach the optimal solution (Tabs. 5 and 6).

3.3 Anechoic structure optimization under hydrostatic pressure

The investigated structure will be subjected to different hydrostatic pressures in actual service. The existing research results show that the hydrostatic pressure has an important influence on the sound absorption coefficient [35]. The water pressure at a depth of 100 m underwater is about 1 MPa. As the water depth of the underwater target structure during normal operation is between 100 and 300 m; the corresponding pressure range were chosen to be 1 MPa, 2 MPa and 3 MPa respectively. Figure 11 shown the sound absorption coefficient under different static pressures. It could be seen that with the increase of static pressure, the overall sound absorption coefficient shows a downward trend, and the high-frequency sound absorption performance becomes worse. This is because under the

action of hydrostatic pressure, the cavity structure and the thickness of the anechoic structure will be compressed. Moreover, the equivalent impedance will fail, which will increase the sound reflection and decrease the sound absorption effect.

In order to further study the optimization problem of the anechoic structure under different hydrostatic pressures; GEK, Kriging model and gradient optimization algorithm were used to optimize the anechoic structure under hydrostatic pressure of 1 MPa, 2 MPa and 3 MPa. The results of the convergence history and sound absorption coefficient under various hydrostatic pressures are shown in Figure 12 and Table 7.

It could be seen from the table that as the hydrostatic pressure increases, the number of sample points required also increases. However, compared to the other two algorithms, GEK increases the sample point by a smaller amplitude. Under 1 MPa, 2 MPa and 3 MPa, the optimization effect of GEK and kriging model was obviously better than that of gradient optimization algorithm. Therefore, it also shown that the surrogate model, especially the GEK surrogate model, has a good effect on noise reduction of the anechoic structure.

From the above discussion, it could be seen in the optimization calculation of the noise reduction structure, The Kriging and GEK models based on the surrogate model can reduce the number of sample points required for gradient optimization by approximately 50% and 70%, respectively. At the same time, it can facilitate parallel optimization design, thereby improving the optimization design efficiency of the silencing structure. Compared with the optimization of the surrogate model in the shape of the wing [36], the advantage of the surrogate model in the anechoic structure has not yet been fully reflected. This is because the optimization dimension of the wing is higher, and the optimization efficiency of the surrogate model will be more obvious.

The optimization of the three working conditions shows that the optimization method based on the proxy model can be used in the field of anechoic structure, but some areas that can be improved in the future are also found in the research:

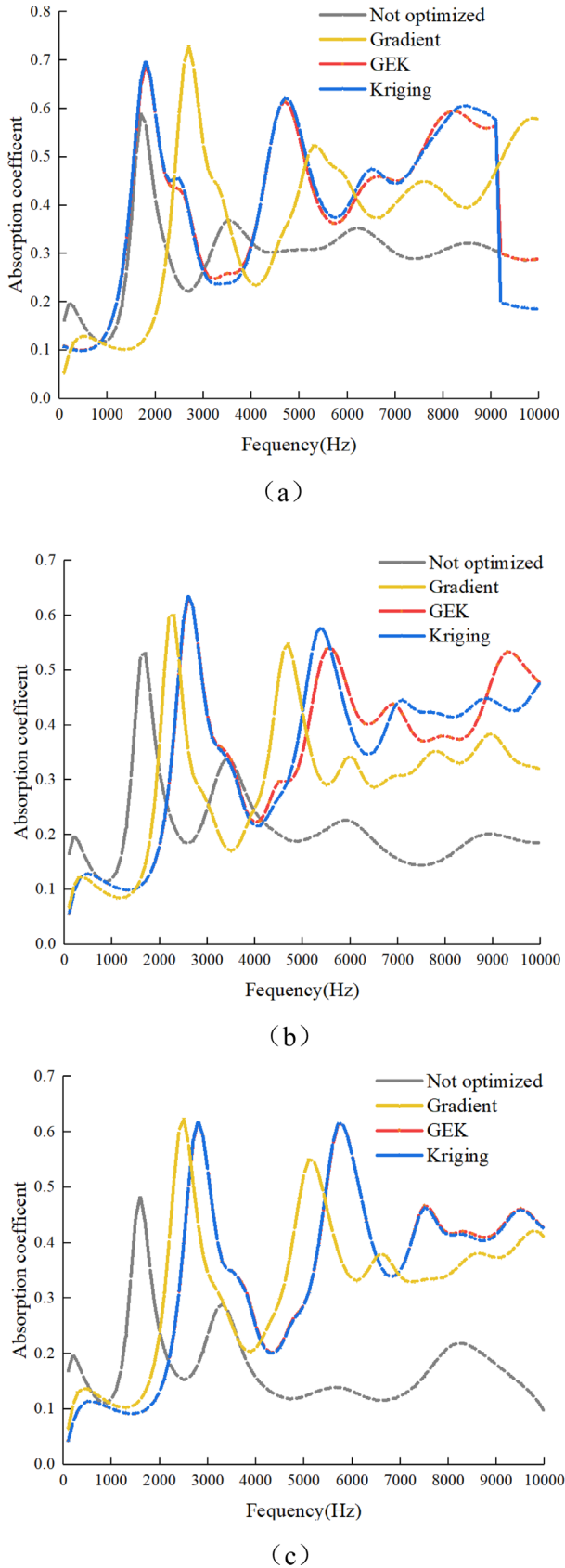


Figure 12. Sound absorption coefficients of different optimization models at different pressures. (a) 1 MPa; (b) 2 MPa; (c) 3 MPa.

1. Develop a variety of cavity structure shape parameterization curves

Before using the optimization method to optimize the design of the silencing structure, it is necessary to use some design parameters to replace the cavity structure, that is, to parameterize the shape of the cavity structure. The conical bus in the article is one of the parameterized curves.

At present, the proxy model can achieve hundreds of dimensions of parameter optimization in the field of wing optimization. Therefore, in future research, we can summarize or propose more parameterized curves to describe the changes in the internal cavity structure, such as new cavities, polygonal cavities, and combined cavity structures to enrich the shape of the cavity structure and explore different shapes. The optimization effect of the cavity structure and its combination.

2. Develop optimized agent models for multiple materials

The silencing material studied in this paper is mainly a combination of iron, rubber, and cavity structure. In the subsequent surrogate model optimization, a variety of materials such as carbon fiber composite material constitutive equation and complex young's model can be considered in the finite element model. Analyze the influence of material parameters on the silencing coefficient by quantitative methods, and develop optimized proxy models for multiple materials.

3. Improve the guidelines for adding points

The core mechanism of agent optimization is the optimization plus point criterion. At present, for low-dimensional optimization problems, the two addition criteria in the article can meet the requirements. When the number of design variables is large, the calculation cost will increase sharply, which reduces the engineering practicability. Therefore, for higher-dimensional problems, additional guidelines need to be further improved.

4. Optimize the GEK model

Although GEK optimization is very good, it also exposes a major problem: in the later stage of the optimization process, the newly added sample points will gather near the optimal value, which will cause the ill-condition of the correlation matrix, which will make the modeling of the proxy model inaccurate. The introduction of gradient information in the model makes the ill-conditioned problem of the correlation matrix more serious. This phenomenon may be one of the reasons that the GEK-based proxy optimization method converges slowly in the later stage of the optimization process.

4 Conclusions

This paper proposes an optimization method for anechoic structure parameters based on surrogate model. The GEK, Kriging, and gradient optimization algorithms were used to optimize and compare the parameter values of the

Table 7. Optimization methods under hydrostatic pressure.

Optimization method	1 MPa		2 MPa		3 MPa	
	Optimization goal	No. of calculations	Optimization goal	No. of calculations	Optimization goal	No. of calculations
Not optimized	0.2987	–	0.2134	–	0.1765	–
Kriging	0.4010	296	0.3500	312	0.3364	342
GEK	0.3957	132	0.3476	144	0.3376	152
Gradient optimization	0.369	497	0.2956	516	0.3221	553

anechoic structure under three working conditions. The following conclusions could be drawn:

1. It is feasible to construct the parameter optimization method of the anechoic structure based on the surrogate model. In the article, by optimizing the conical bus bar and using two parallel dot addition criteria, a 10-dimensional anechoic structure shape parameter and material parameter optimization design method was successfully constructed. This method can also be applied to the optimization of other cavity shapes and composite materials. The optimization results show that: compared with the gradient optimization algorithm, the proxy model can significantly reduce the number of model calculations, and the optimization effect is better.
2. Under the assumption that the calculation cost of the gradient is the same as the calculation cost of the objective function, the optimization results of GEK and Kriging surrogate models are similar, but GEK used less time and converges faster.
3. In different working conditions, the optimal structure is not universal. In the full-frequency optimization condition, when the operating frequency is greater than 2000 Hz, the optimization effect is more obvious than that at less than 2000 Hz. In the low-frequency condition, the anechoic structure and the physical parameters work together. Under static pressure deformation, the muffling coefficient is inversely proportional to the hydrostatic pressure, and the optimization effect of GEK and Kriging models at 1 MPa, 2 MPa and 3 MPa is significantly better than the gradient optimization algorithm.

Author contributions

Conceptualization, H.S. and X.W.; methodology, H.S.; validation, H.S. and L.S.; formal analysis, J.S.; investigation, H.S.; resources, L.S.; data curation, L.S.; writing – original draft preparation, H.S.; writing – review and editing, X.W.; visualization, X.W.; supervision, H.S.; project administration, H.S. All authors have read and agreed to the published version of the manuscript.

Funding

This research was funded by the national defense science and technology innovation zone project; grant number 19-163-13-ZD-024-003-02.

Conflicts of interest

The authors declare no conflict of interest. The funders had no role in the design of the study; in the collection, analyses, or interpretation of data; in the writing of the manuscript, or in the decision to publish the results.

Acknowledgments

The authors would like to thank Prof. Yuan He from Systems Engineering Research Institute. Finally, we would like to thank the anonymous reviewers for the insightful comments and helpful suggestions made.

References

1. X.Y. He, Z.M. Cai, J.Y. Lin, X.Z. Jiang, H.N. Huang: The simulation research on forecasting the detection range of active sonar. *Acta Simulata Systematica Sinica* 15, 9 (2003) 1304–1306. <https://doi.org/10.3969/j.issn.1004-731X.2003.09.030>.
2. S.M. Ivansson: Numerical modeling for design of viscoelastic coatings with favorable sound absorbing properties. *Nonlinear Analysis: Theory, Methods & Applications* 30, 63 (2005) 1541–1550. <https://doi.org/10.1016/j.na.2005.01.050>.
3. S.M. Ivansson: Sound absorption by viscoelastic coatings with periodically distributed cavities. *The Journal of the Acoustical Society of America* 119, 6 (2006) 3558–3567. <https://doi.org/10.1121/1.2190165>.
4. H.C. Strifors, G.C. Gaunard: Selective reflectivity of viscoelastically coated plates in water. *The Journal of the Acoustical Society of America* 88, 2 (1990) 901–910. <https://doi.org/10.1121/1.399741>.
5. M.K. Hinders, B.A. Rhodes, T.M. Fang: Particle-loaded composites for acoustic anechoic coatings. *Journal of Sound and Vibration* 185, 2 (1995) 219–246. <https://doi.org/10.1006/jsvi.1995.0377>.
6. H.G. Zhao, Y.Z. Liu, J.H. Wen, D.L. Yu, G. Wang: Sound absorption of locally resonant sonic materials. *Chinese Physics Letters* 23, 008 (2006) 2132. <https://doi.org/10.1088/0256-307X/23/8/047>.
7. G.A. Brigham, J.J. Libuha, R.P. Radlinski: Analysis of scattering from large planar gratings of compliant cylindrical shells. *Journal of the Acoustical Society of America* 61, 1 (1977) 48–59. <https://doi.org/10.1121/1.381267>.
8. R.P. Radlinski: Scattering from multiple gratings of compliant tubes in a viscoelastic layer. *Journal of the Acoustical Society of America* 85, 6 (1989) 2301–2310. <https://doi.org/10.1121/1.397776>.
9. B. Liang, X. Zou, J. Cheng: Effective medium method for sound propagation in a soft medium containing air bubbles. *Journal of the Acoustical Society of America* 124, 3 (2008) 1419. <https://doi.org/10.1121/1.2957931>.

10. M. Hao, J. Wen, H. Zhao, X. Wen: Optimization of locally resonant acoustic metamaterials on underwater sound absorption characteristics. *Journal of Sound and Vibration* 331, 20 (2012) 4406–4416. <https://doi.org/10.1016/j.jsv.2012.05.027>.
11. A.C. Hennion, R. Bossut, J.N. Decarpigny: Analysis of the scattering of a plane acoustic wave by a periodic elastic structure using the finite element method: Application to compliant tube gratings. *The Journal of the Acoustical Society of America* 87, 4 (1990) 1861–1870. <https://doi.org/10.1121/1.399312>.
12. A.C. Hennion, J.N. Decarpigny: Analysis of the scattering of a plane acoustic wave by a doubly periodic structure using the finite element method: Application to Alberich anechoic coatings. *The Journal of the Acoustical Society of America* 90, 6 (1991) 3356–3367. <https://doi.org/10.1121/1.401395>.
13. V. Easwaran, M.L. Munjal: Analysis of reflection characteristics of a normal incidence plane wave on resonant sound absorbers: A finite element approach. *Journal of the Acoustical Society of America* 93, 3 (1993) 1308–1318. <https://doi.org/10.1121/1.405416>.
14. J. Zhong, H.G. Zhao, H.B. Yang, J.F. Yin, J.H. Wen: On the accuracy and optimization application of an axisymmetric simplified model for underwater sound absorption of anechoic coatings. *Applied Acoustics* 145 (2019) 104–111. <https://doi.org/10.1016/j.apacoust.2018.10.005>.
15. J.V. Ramakrishnan, L.R. Koval: A finite element model for sound transmission through laminated composite plates. *Journal of Sound & Vibration* 112, 3 (1987) 433–446. [https://doi.org/10.1016/S0022-460X\(87\)80109-8](https://doi.org/10.1016/S0022-460X(87)80109-8).
16. P. Gerstoft: Inversion of seismoacoustic data using genetic algorithms and a posteriori probability distributions. *Journal of the Acoustical Society of America* 95, 2 (1994) 770–782. <https://doi.org/10.1121/1.408387>.
17. V. Westerlin: Multi-frequency inversion of synthetic transmission loss data using a genetic algorithm. *Journal of Computational Acoustics* 6, 01n02 (2011) 205–221. <https://doi.org/10.1142/S0218396X98000156>.
18. S.M. Ivansson: Numerical design of Alberich anechoic coatings with superellipsoidal cavities of mixed sizes. *Journal of the Acoustical Society of America* 124, 4 (2008) 1974–1984. <https://doi.org/10.1121/1.2967840>.
19. Y.C. Chang, L.J. Yeh, M.C. Chiu: Optimization of constrained composite absorbers using simulated annealing. *Applied Acoustics* 66, 3 (2005) 341–352. <https://doi.org/10.1016/j.apacoust.2004.07.003>.
20. M. Tao, Y. Zhao, G.W. Wang: Parameter optimization of sound absorption layer based on genetic algorithm. *Journal of Vibration & Shock* 33, 2 (2014) 20–25. <https://doi.org/10.3969/j.issn.1000-3835.2014.02.004>.
21. D.G. Krige: A statistical approach to some basic mine valuation problems on the Witwatersrand. *Journal of the Southern African Institute of Mining and Metallurgy* 52, 6 (1951) 119–139. https://hdl.handle.net/10520/AJA0038223X_4792.
22. J. Sacks, W.J. Welch, T.J. Mitchell: Design and analysis of computer experiments. *Statistical Science* 4, 4 (1989) 409–435. <https://www.jstor.org/stable/2245858>.
23. X.F. Mu, W.X. Yao, X.Q. Yu: A survey of surrogate models used in MDO. *Chinese Journal of Computational Mechanics* 22, 5 (2005) 608–612. http://en.cnki.com.cn/Article_en/CJFDTOTAL-JSJK200505018.htm.
24. A.I.J. Forrester, A. Sobster, A.J. Keane: Engineering design via surrogate modeling: A practical guide. John Wiley & Sons, Chichester, 2008. ISBN: 978-0-470-06068-1.
25. A. Vavalle, N. Qin: Iterative response surface based optimization scheme for transonic airfoil design. *Journal of Aircraft* 44, 2 (2007) 365–376. <https://doi.org/10.2514/1.19688>.
26. H. Yan, G. Zhu, Z. Xu, S. Gao: Volume rendering and 3D modeling of hydrologic layer based on Kriging algorithm. *Journal of Wuhan University, Information Science Edition* 29, 7 (2004) 611–614. <https://doi.org/10.13203/j.whugis2004.07.011>.
27. P. Eguía, E. Granada, J.M. Alonso: Weather datasets generated using Kriging techniques to calibrate building thermal simulations with TRNSYS. *Journal of Building Engineering* 7 (2016) 78–91. <https://doi.org/10.1016/j.jobee.2016.05.007>.
28. Z.H. Han, S. Görtz, R. Zimmermann: Improving variable-fidelity surrogate modeling via gradient-enhanced kriging and a generalized hybrid bridge function. *Journal of Aerospace Science and Technology* 25, 1 (2013) 177–189. <https://doi.org/10.1016/j.ast.2012.01.006>.
29. Z.H. Han, R. Zimmermann, S. Görtz: Alternative cokriging model for variable-fidelity surrogate modeling. *AIAA Journal* 50, 5 (2012) 1205–1210. <https://doi.org/10.2514/1.J051243>.
30. Z.H. Han, S. Görtz, R. Hain: A variable-fidelity modeling method for aero-loads prediction. *New Results in Numerical and Experimental Fluid Mechanics VII, Notes on Numerical Fluid Mechanics and Multidisciplinary Design* 112 (2010) 17–25. https://doi.org/10.1007/978-3-642-14243-7_3.
31. Z.Y. He, M. Wang: Investigation of the sound absorption of homogeneous composite multiple-layer structures in water. *Applied Acoustics* 15, 5 (1996) 6–11. <https://doi.org/JournalArticle/5af134acc095d718d8df6ee8>.
32. J. Sun: Design theory and realization of low-frequency sound source based on water gap discharge. Ph.D. Thesis, Dalian University of Technology Library, Dalian, 2010.
33. C. Ren: Acoustic performance analysis and optimal design of sound absorbing cover and composite acoustic panel. Doctoral dissertation, Dalian University of Technology, Dalian, Liaoning, China, 2020.
34. T. Meng: Simplified model for predicting acoustic performance of an underwater sound absorption coating. *Journal of Vibration & Control* 20, 3 (2014) 339–354.
35. M. Zadkarami, M. Shahbazian, K. Salahshoor: Pipeline leakage detection and isolation: An integrated approach of statistical and wavelet feature extraction with multi-layer perceptron neural network (MLPNN). *Journal of Loss Prevention in the Process Industries* 43 (2016) 479–487.
36. S.N. Panigrahi, C.S. Jog, M.L. Munjal: Multi-focus design of underwater noise control linings based on finite element analysis. *Applied Acoustics* 69, 12 (2008) 1141–1153. <https://doi.org/10.1016/j.apacoust.2007.11.012>.

Cite this article as: Song H. Su L. Yan X. & Liu J. 2022. An optimization method for material sound absorption performance based on surrogate model. *Acta Acustica*, 6, 22.